

# Stereo Anything: Unifying Stereo Matching with Large-Scale Mixed Data

Xianda Guo<sup>1,\*</sup>, Chenming Zhang<sup>2,3,\*</sup>, Youmin Zhang<sup>4,5</sup>, Dujun Nie<sup>6</sup>, Ruilin Wang<sup>6</sup>,  
Wenzhao Zheng<sup>7</sup>, Matteo Poggi<sup>4</sup>, Long Chen<sup>6,2,3,†</sup>

<sup>1</sup> School of Computer Science, Wuhan University

<sup>2</sup> Institute of Artificial Intelligence and Robotics, Xi'an Jiaotong University

<sup>3</sup> Waytous <sup>4</sup> University of Bologna <sup>5</sup> Rock Universe

<sup>6</sup> Institute of Automation, Chinese Academy of Sciences <sup>7</sup> University of California, Berkeley

<https://github.com/XiandaGuo/OpenStereo>

xianda\_guo@163.com; chmzhang@outlook.com

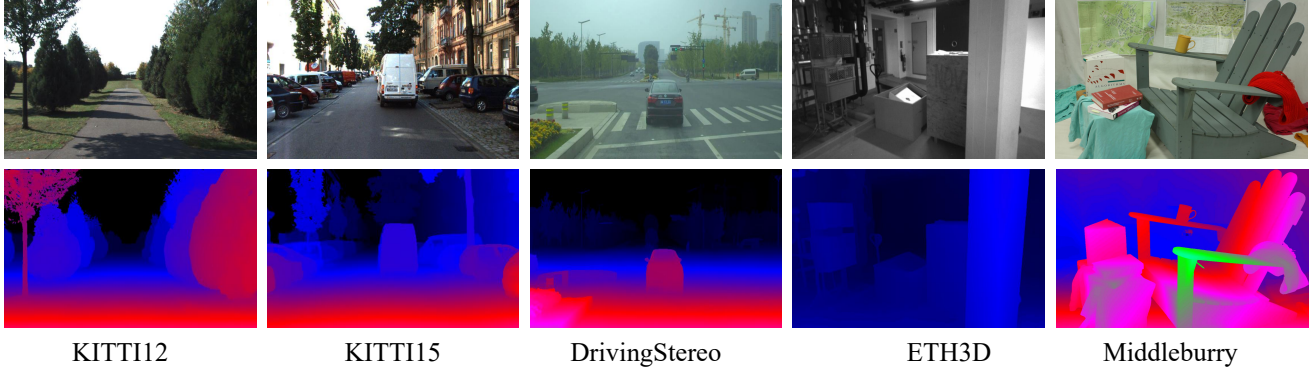


Figure 1. StereoAnything demonstrates impressive generalization capabilities in different unseen scenes.

## Abstract

*Stereo matching has been a pivotal component in 3D vision, aiming to find corresponding points between pairs of stereo images to recover depth information. In this work, we introduce StereoAnything, a highly practical solution for robust stereo matching. Rather than focusing on a specialized model, our goal is to develop a versatile foundational model capable of handling stereo images across diverse environments. To this end, we scale up the dataset by collecting labeled stereo images and generating synthetic stereo pairs from unlabeled monocular images. To further enrich the model’s ability to generalize across different conditions, we introduce a novel synthetic dataset that complements existing data by adding variability in baselines, camera angles, and scene types. We extensively evaluate the zero-shot capabilities of our model on five public datasets, showcasing its impressive ability to generalize to new, unseen data (Figure 1).*

\*These authors contributed equally to this work.

†Corresponding authors

## 1. Introduction

Computer vision is currently undergoing a revolution due to the development of foundation models in object recognition [43], image segmentation [21], and monocular depth estimation [19, 31, 49, 50], which demonstrate strong zero- and few-shot performance across various downstream tasks. Stereo matching is fundamental for enabling depth perception and 3D reconstruction of observed scenes, playing a critical role in applications such as robotics [56], autonomous driving [15, 16], and augmented reality [47]. However, the exploration of foundation models in stereo matching remains limited due to the extreme difficulty of obtaining accurate disparity ground truth (GT) data. Although numerous stereo datasets [11, 18, 27, 29, 48] have been published, fully leveraging these datasets for training is challenging. Moreover, these annotated datasets are insufficient to train an ideal foundation model even when combined.

Stereo-from-mono [44] is a pioneer study that aimed to generate stereo image pairs and disparity maps directly from monocular images to overcome those challenges. However, this approach resulted in the creation of only

500,000 data samples, which is relatively limited considering the scale required to train robust foundation models effectively. While this effort represents an important step towards reducing the dependency on expensive stereo data collection, the generated dataset is still insufficient for building large-scale models capable of generalizing well to diverse real-world conditions.

In this work, we introduce StereoAnything, a foundation model for stereo matching aimed at providing high-quality disparity estimation for any pair of rectified stereo images, regardless of scene complexity or environmental conditions. Our primary focus is on creating a highly generalized and scalable solution capable of handling diverse scenarios. To achieve this ambitious goal, we adopt a strategy centered on significantly scaling up the training dataset, ensuring that the model is exposed to an extensive variety of scenes. To fully leverage the existing stereo datasets, we utilize numerous publicly available annotated stereo datasets as a core part of our training data, as well as create a new synthetic dataset, *StereoCarla*, to further increase the quality, quantity and variety of training data available. Furthermore, inspired by the successes of the stereo-from-mono [44] approach and the new monocular depth foundation models [19, 31, 49, 50], we supplement our training with a large volume of synthetic stereo data generated from monocular images. By combining both traditional stereo datasets and newly generated monocular-based stereo pairs, we create a diverse and comprehensive training set that allows StereoAnything to excel in various environments, ensuring robust and accurate depth predictions. This integration of both real and synthetic data helps us overcome limitations related to data scarcity, ultimately pushing the boundaries of stereo-matching capabilities and improving generalization across domains.

Our contributions can be summarized as follows:

- We first emphasize the importance of scaling up labeled stereo datasets, through an exhaustive study on how different synthetic datasets affect the performance of trained stereo models.
- Then, we build a new synthetic dataset to better generalize across different scenarios and enhance the performance, called StereoCarla. Compared to existing datasets, it features unique view angles and baselines.
- We further scale up the training data by effectively incorporating both synthetic stereo data and diverse unlabeled monocular images for training stereo networks.
- Our final dataset allows for training a stereo model to exhibit the strongest zero-shot capability among all of the existing networks.

## 2. Related Work

Stereo matching has been extensively studied in the last decade. We identify and review two main bodies of litera-

ture, concerning in-domain and cross-domain stereo matching, as well as review techniques for multi-dataset training.

### 2.1. In-domain Stereo Matching

Early methods depended on hand-crafted features and optimization-based matching [17, 33]. With the rise of deep learning, the CNN-Based model [6, 14, 20, 55] has revolutionized stereo matching by learning feature representations and matching costs directly from data, leading to significant improvements in accuracy and robustness. GCNet [20] firstly constructs concatenation-based 4D cost volumes and utilizes 3D CNNs for cost aggregation. Based on GCNet, PSMNet [6] enhances feature extraction using a spatial pyramid pooling module and employs a stacked hourglass architecture for 3D cost aggregation. GANet [54] accelerates the network by replacing the 3D CNN with a semi-global aggregation layer and a local guided aggregation layer. LEAStereo [9] employs neural architecture search to optimize stereo-matching networks. Recently, there has been a growing interest in video stereo matching [18, 53, 59], particularly in leveraging temporal information to achieve consistent stereo matching. Despite their success, these approaches often exhibit domain-specific biases, limiting their performance on unseen datasets.

### 2.2. Cross-domain Stereo Matching

Domain-invariant representations are crucial for cross-domain stereo matching. Tonioni *et al.* [37] propose an unsupervised adaptation method that can fine-tune a stereo-matching model without any ground-truth information. DSMNet [55] incorporates a trainable non-local graph filter and domain normalization layer to extract robust structural features. CFNet [36] addresses the large domain difference by introducing a cascade and fused cost volume. FCStereo [57] proposes contrastive learning to maintain feature consistency between matching pixels, which is vital for the generalization of stereo matching. To reduce domain shifts, Chang *et al.* [8] presents a hierarchical visual transformation network that focuses on learning shortcut-invariant representation from synthetic data. RAFT-Stereo [24] and IGEV [46] introduce multi-level ConvGRUs to update the disparity map and achieve strong cross-dataset generalization iteratively. MS-Net [5], GraftNet [25], and FormerStereo [60] obtain domain-invariant features by leveraging external priors and employing robust feature extractors. The primary difference is that MS-Net [5] and GraftNet [25] focus on CNN backbones, while FormerStereo [60] employs a ViT-based foundational model. NMRF-Stereo [13] presents a neural MRF model, which exhibits strong cross-domain generalization and can recover sharp edges. Zhang *et al.* [58] explores fine-tuning stereo-matching networks in a manner that preserves their robustness to unseen domains and harnesses the discrepan-

Dataset	Published	Indoor	Outdoor	Dynamic	Video	Dense	Accuracy	Diversity	Annotation	Baseline	FL	Range	Ave./Med.	# images
Sintel [3]	ECCV2012	✓	✓	✓	✓	✓	High	Medium	Synthetic	0.1m	-	0-972	66.5/25	1,064
SceneFlow [27]	CVPR2016	✓	✓	✓	✓	✓	High	High	Synthetic	0.54m	-	0-10501	53.9/36	35,454
FallingThings [40]	CVPRW2018	✓	✓	✗	✗	✓	High	Low	Synthetic	6cm	768.2px	7-461	35.2/34	61,500
Argoverse [7]	CVPR2019	✗	✓	✓	✓	✓	Low	Low	LiDAR	-	-	0-256	69.1/59	5,530
VirtualKITTI2 [4]	ArXiv2020	✗	✓	✓	✓	✓	High	Mid	Synthetic	0.53m	725px	0-411	30.1/25	21,260
Tartanair [42]	IROS2020	✓	✓	✓	✓	✓	High	High	Synthetic	-	-	0-499	21.0/13	306,637
InStereo2K [2]	SCIS2020	✓	✗	✗	✗	✗	Low	Low	LiDAR	10cm(5cm)	8mm	0-328	78.4/74	2,010
UnrealStereo4K [38]	CVPR2021	✓	✓	✗	✗	✓	High	High	Synthetic	0.2m(0.5m)	-	0-1515	175.3/135	8,200
CREStereo [23]	CVPR2022	✓	✓	✗	✗	✓	High	High	Synthetic	-	-	0-2048	15.2/8	200,000
Spring [28]	CVPR2023	✗	✓	✓	✓	✓	High	Low	Synthetic	6.5cm	-	0-554	38.1/19	5,000
DynamicStereo [18]	CVPR2023	✓	✗	✓	✓	✓	High	Low	Synthetic	4cm-30cm	-	3-35,097	62.7/48	144,900
StereoCarla (Ours)	-	✗	✓	✓	✓	✓	High	High	Synthetic	10cm,54cm,100cm,200cm,300cm	10m	0-2644	75.7/31	552,050
KITTI12 [11]	CVPR2012	✗	✓	✓	✓	✗	Medium	Low	LiDAR	0.54m	720px	4-232	40.1/38	194
Middlebury [34]	GCPR2014	✓	✗	✗	✗	✗	High	Low	LiDAR	140-400mm	1100px-3600px	15-323	72.5/63	15
KITTI15 [29]	CVPR2015	✗	✓	✓	✓	✗	Medium	Low	LiDAR	0.54m	520px	4-230	35.2/33	200
ETH3D [35]	CVPR2017	✓	✓	✗	✓	✗	High	Low	LiDAR	59.5mm-60.4mm	529px-712px	0-62	13.7/10	27
DrivingStereo [48]	CVPR2019	✗	✓	✓	✓	✗	Low	High	LiDAR	0.54m	1003	4-128	31.0/26	7,751

Table 1. **Datasets used in our work.** Top: Our training sets. Bottom: Our test sets. FL refers to focal length. Ave./Med. refers to the average/median of disparity. Range refers to disparity range.

cies between ground truth data and pseudo labels to extract valuable insights for the fine-tuning process.

We refer the reader to recent surveys [22, 30, 39] for further details on both in-domain and cross-domain stereo.

### 2.3. Multi-Dataset Training

To tackle the challenge of generalization, some researchers have increasingly explored multi-dataset training strategies. By combining multiple datasets, models can be trained to capture diverse scene characteristics better, making them more robust. Although well-established in fields like object recognition [43], segmentation [21], and monocular depth estimation [19, 31, 49, 50], the use of this strategy in stereo matching remains relatively underexplored.

In this work, we introduce StereoAnything, a stereo-matching model that systematically leverages multi-dataset learning. Inspired by the successes in related domains, we aim to enhance the generalization capabilities of stereo-matching models by training on a diverse collection of datasets. By doing so, we seek to develop a model that performs consistently across any conditions.

## 3. Existing Datasets

We start by revising existing labeled stereo datasets, and unlabeled monocular datasets. Table 1 summarizes the existing labeled datasets involved in our work, dividing them into training and testing sets, along with their properties.

### 3.1. Training datasets.

#### 3.1.1 Labeled stereo datasets.

To fully leverage the existing stereo datasets, we utilize numerous publicly available annotated stereo datasets as a core part of our training data.

**Sintel** [3], sourced from computer-generated films and providing dense ground-truth labels, is separated by training datasets (1,064 stereo pairs) and tests (564 stereo pairs).

**SceneFlow** [27] is a synthetic dataset comprising indoor and outdoor scenes. It is one of the most commonly used datasets in stereo matching, providing valuable ground truth for pre-train stereo-matching algorithms.

**CREStereo** [23] focuses on challenging scenarios in real-world scenes by incorporating various types of lighting conditions with random colors and luminance at different positions.

**FallingThings** [40] is a large-scale synthetic dataset designed to advance research in 3D object detection and pose estimation, also providing annotated stereo images.

**InStereo2K** [2] introduces a dataset of over 2,000 real-world, indoor stereo image pairs with high-quality, semi-dense ground-truth disparities.

**Spring** [28] provides 6,000 high-resolution image pairs, each with a 2.1 Mpx resolution, spanning 47 diverse scenes.

**UnrealStereo4K** [38] is a high-resolution, synthetic stereo dataset, including 8Mpx stereo pairs.

**Argoverse** [7] is a dataset for 3D tracking and motion forecasting. It contains 5,530 forward-facing stereo images for training and 1,094 for testing with a resolution of  $2056 \times 2464$ , collected in real driving environments.

**VirtualKITTI2** [4] employs advancements in Unity’s lighting and post-processing techniques to generate a dataset with minimal differences between generated and real images from KITTI. It includes 21,260 stereo pairs.

**Tartanair** [42] is a large-scale synthetic dataset specifically designed to advance the development of Visual SLAM. It offers a diverse range of simulated environments with varying lighting conditions, weather effects, and dynamic objects, which includes 306,637 stereo pairs.

**DynamicStereo** [18] distinguishes among others for its extended sequences and the presence of non-rigid objects such as animals and humans. The dataset comprises 484/20/20 sequences for training/validation/testing.



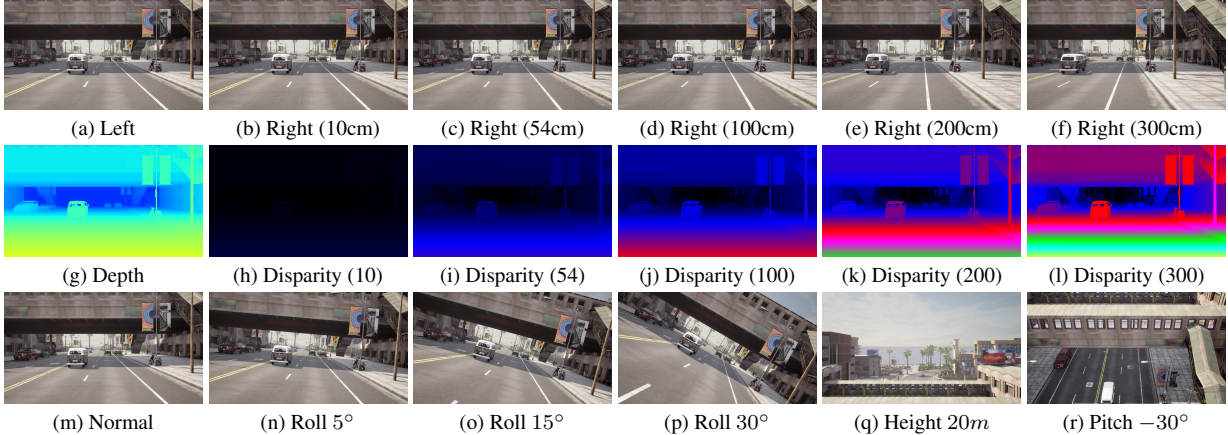


Figure 2. **Overall of StereoCarla datasets.** The first row illustrates the left-eye image (1st column) and the right-eye image at varying baselines (2nd - 6th columns). The second row showcases the depth map (1st column) and corresponding disparity maps (2nd - 6th columns). The third rows depict left images from varied horizontal viewing angles and elevated viewpoints.

Dataset	Indoor	Outdoor	# Images
LSUN [51]	✓		9.8M
ImageNet-21K [32]	✓		13.1M
BDD100K [52]		✓	0.1M
Google Landmarks [45]		✓	4.97M
Places365 [61]	✓	✓	2.1M

Table 2. **Unlabeled monocular images.** M refers to million.

### 3.1.2 Unlabeled monocular datasets.

To enhance the robustness of the stereo-matching model, we incorporate a large-scale collection of 30.07 million unlabeled monocular images sourced from four public datasets. A comprehensive overview of these datasets is provided in Table 2. These will be used to generate further, synthetic stereo pairs during training.

### 3.2. Testing datasets.

To evaluate the zero-shot generalization performance of the stereo-matching model, we select five datasets known for their diversity and accurate ground truth annotations.

**KITTI 2012** [11] and **KITTI 2015** [29] datasets are widely used benchmarks in stereo matching with sparse LiDAR ground truth disparities, featuring real-world images captured from various driving scenarios. KITTI 2012 [11] includes 194 training and 195 testing pairs, while KITTI 2015 [29] has 200 training and 200 testing pairs.

**Middlebury** [34] focus on indoor environments, offering 15/15 high-resolution stereo pairs for training and testing annotated with semi-dense ground-truth labels obtained with a structured light system.

**ETH3D** [35] has 27/20 grayscale stereo image pairs for training and testing, collected from both indoor and outdoor scenes, annotated with semi-dense ground-truth labels obtained with a Faro Focus X 330 laser scanner.

**DrivingStereo** [48] is a large-scale stereo dataset that includes over 180K images covering a diverse set of real-world driving scenarios. Sparse ground-truth annotations are obtained from LiDAR scans, being post-processed through a deep neural network.

## 4. StereoCarla Datasets

To expand the diversity and quantity of existing stereo-matching datasets, we utilized the CARLA [10] simulator to collect new synthetic stereo data. CARLA [10], a widely used open-source simulator for autonomous driving research, enabled us to create a range of realistic virtual environments, which significantly increased the flexibility of our data collection process. Compared to previous stereo datasets, our approach offers more varied settings, providing different baselines and novel camera configurations that enhance the richness of stereo data. And Figure 2 illustrates some examples of the newly collected dataset, showcasing the diverse baselines, camera angles, and scene variations. Below, we detail the major design considerations:

**Multiple Baselines.** We collected data with baseline distances set at 10 cm, 54 cm, 100 cm, 200 cm, and 300 cm, which are much broader in range compared to existing datasets. These baseline variations allow the model to better generalize to scenarios where the distance between the two cameras can differ greatly, such as switching between different hardware configurations in real-world applications.

**Horizontal Viewing Angles.** We collected data at four different horizontal viewing angles. Specifically, we captured images at a direct horizontal view (0 degrees) and slight and moderate rotations of 5 degrees, 15 degrees, and 30 degrees. These different orientations provide more robust data, as they simulate variations that occur naturally when a stereo camera system is in motion or when changes in scene viewpoint occur. This kind of angular variation is



crucial for enhancing the robustness of a model, making it more resilient to real-world shifts in perspective.

**Elevated Viewpoints.** Furthermore, to simulate a diverse set of environments and perspectives, we positioned the stereo camera pair at an elevated height of 10 meters above the vehicle, capturing the scenes from both a horizontal view and at a 30-degree downward tilt. This unique perspective provides more information about the overall layout of the scene, which can be particularly useful in understanding both near-ground details and broader contextual elements that are missing in most existing datasets.

**High Resolution.** Each scene in our dataset consists of left and right images, with a resolution of  $1600 \times 900$  pixels, along with corresponding dense disparity maps, ensuring comprehensive ground-truth information for both training and evaluating state-of-the-art stereo models.

By incorporating the above elements, our dataset aims to address key limitations in existing stereo datasets, particularly the lack of varied viewpoints and baseline distances, thereby providing a more robust foundation for developing and testing stereo-matching algorithms.

## 5. StereoAnything

We now introduce our framework, StereoAnything, designed for training a robust stereo network by using large-scale mixed data.

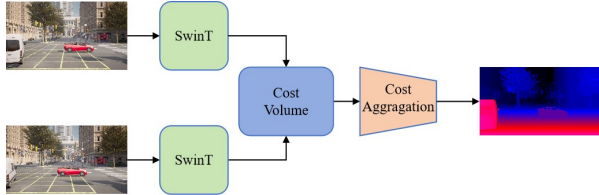


Figure 3. **Stereo Matching Pipeline.** Deep stereo models usually perform feature extraction, cost construction, cost aggregation, and disparity regression.

### 5.1. Pipeline of Stereo Matching

As shown in Figure 3, stereo matching based on deep learning involves estimating disparity from a pair of rectified stereo images. It mainly consists of four essential components [6, 13, 39]: feature extraction, cost construction, cost aggregation, and disparity regression.

### 5.2. Learning Labeled Stereo Images

In this section, we describe our approach to enhancing stereo model generalization by leveraging supervised stereo data. It is important to note that monocular depth models like MiDaS [31], DepthAnythingV1 [49], and DepthAnythingV2 [50] normalize the depth values to a range of 0 to 1 on each depth map. However, this normalization is clearly

unsuitable for stereo matching, as stereo matching has inherent scale information that would be lost during the process.

Our method begins by training the stereo model on a single dataset and subsequently evaluating its generalization performance across test datasets. To quantify the generalization ability, we calculate the mean metric across these five datasets, producing a ranking of datasets that allows us to assess their impact on cross-dataset performance:

$$P_{r_1} = f_{eval}(M, D_1) \quad (1)$$

Next, we rank all datasets based on evaluation metrics:

$$\{D_{r_1}, D_{r_2}, \dots, D_{r_n}\}, \text{ such that } P_{r_1} \geq P_{r_2} \geq \dots \geq P_{r_n} \quad (2)$$

The datasets are ranked from highest to lowest performance.

The mixing process starts with the top-ranked dataset  $D_{r_1}$ , and we sequentially add other datasets to the mixed training set based on their ranking. This approach ensures that the training process incorporates data that is most beneficial to improving generalization performance, ultimately yielding a model that is more robust when applied to various unseen stereo datasets:

$$MIX_k = \bigcup_{i=1}^k D_{r_i}, \quad \text{where } k \in \{1, 2, \dots, n\} \quad (3)$$

By employing this incremental combination strategy, we aim to exploit the diversity of multiple datasets while ensuring that the highest-quality data is prioritized during training.

### 5.3. Learning Stereo from Single Images

This process is similar to work [44]. Given a single color image  $I$ , a pre-trained monocular depth estimation model  $g$  is used to estimate the depth  $Depth$  of image  $I$ :

$$Depth = g(I) \quad (4)$$

Next, we need to convert the estimated depth  $Z$  into a disparity map  $\tilde{D}$ . For simulating realistic stereo pairs with varied baselines and focal lengths, the disparity  $\tilde{D}$  is calculated as follows:

$$\tilde{D}_{isp} = \frac{s \times Depth_{\max}}{Depth} \quad (5)$$

where  $s$  is a scaling factor randomly sampled from a uniform distribution  $[disp_{\min}, disp_{\max}]$ , ensuring that the disparities lie within a plausible range.

The goal is to synthesize a new ‘right’ image  $\tilde{I}_r$  from the original image  $I_l$  and the predicted disparity  $\tilde{D}_{isp}$ . Unlike backward warping, forward warping is applied here to

generate  $\tilde{I}_r$ , by translating each pixel  $i$  in  $I_l$  by  $Disp_i$  to the left. This approach requires interpolation for filling in missing values and involves challenges such as occlusion handling and pixel collisions.

Finally, we need to handle occlusions and collisions. During forward warping, certain regions in the right image  $\tilde{I}_r$  may remain unfilled due to occlusion, resulting in unnatural gaps. To mitigate this, we use textures from a randomly selected image  $I_b$  in our dataset to fill in the missing pixels. We perform color transfer between  $I_l$  and  $I_b$  to match their visual properties before filling.

## 6. Experiment

We now evaluate the performance achieved by a state-of-the-art stereo model trained within StereoAnything.

### 6.1. Implementation Details

Our experiments are conducted based on OpenStereo [15]. We adopt NMRF-Stereo [13] as our baseline model due to its strong performance and speed in stereo matching. SwinTransformer [26] is adopted for feature extraction. AdamW optimizer is used for training. For pretraining on SceneFlow [27], we utilize OneCycleLR scheduling with a maximum LR of 0.001, while fine-tuning on other datasets uses OneCycleLR with a maximum LR of 0.0005. The batch size is consistently set to 16 across all experiments. For fine-tuning on different single training sets, we train the model for a total of 31,250 iterations. When fine-tuning on mixed datasets, we extend the training to 81,000 iterations to allow the model to effectively learn from the combined data. For fine-tuning on pseudo stereo datasets, we train the model for one epoch, due to the large amount of data. Data augmentation techniques, including color jitter and random erasing, are applied to enhance the robustness of the model.

### 6.2. Test datasets and metrics.

For all experiments, we evaluate our method on five benchmark datasets: KITTI2012 [11] (194 training image pairs), KITTI2015 [29] (200 training image pairs), Middlebury [34] (15 image pairs), ETH3D [35] (27 image pairs), and DrivingStereo [48] (7,751 image pairs). Middlebury [34] is tested on half-resolution. Following recent works [46, 55], we use the D1-all metric for KITTI2012 [11], KITTI2015 [29], and DrivingStereo [48], Bad 2.0 for Middlebury [34], and Bad 1.0 for ETH3D [35]. The D1-all computes the percentage of pixels with an absolute disparity error larger than 3.0 pixels. Bad 1.0/Bad 2.0 metric measures the percentage of pixels with a disparity error greater than 1.0/2.0 pixel.

### 6.3. Comparison with other SOTA methods

As shown in Table 3, we compare our best-performing model with several SOTA stereo-matching methods.

Method	K12	K15	Midd	E3D	DR	Mean
PSMNet [6]	30.51	32.15	33.53	18.02	36.19	30.08
CFNet [36]	13.64	12.09	23.91	7.67	27.26	16.91
GwcNet [14]	23.05	25.19	29.87	14.54	35.40	25.61
COEX [1]	12.08	11.01	25.17	11.43	24.17	16.77
FADNet++ [41]	11.31	13.23	24.07	22.48	20.50	18.32
Cascade [12]	11.86	12.06	27.39	11.62	27.65	18.12
LightStereo-L	6.41	6.40	17.51	11.33	21.74	12.68
IGEV [46]	4.88	5.16	8.47	3.53	<b>6.20</b>	5.67
StereoBase [15]	4.85	5.35	9.76	3.12	11.84	6.98
NMRFStereo [13]	<b>4.20</b>	5.10	7.50	3.80	11.92	6.50
NMRFStereo [13]*	8.67	7.46	16.36	23.46	34.58	18.11
<b>StereoAnything</b>	4.29	<b>4.31</b>	<b>6.96</b>	<b>1.84</b>	7.64	<b>5.01</b>

Table 3. **Comparison with SOTA methods** on KITTI12 [11], KITTI15 [29], Middlebury [34], ETH3D [35], and DrivingStereo [48]—lower is better. NMRFStereo\* refers to NMRFStereo-SwinT. **Bold: Best.**

Method	K12	K15	Midd	E3D	DR	Mean
LightStereo-L	6.41	6.40	17.51	11.33	21.74	12.68
LightStereo-L <sup>†</sup>	<b>4.29</b>	<b>5.82</b>	<b>9.5</b>	<b>5.10</b>	<b>9.44</b>	<b>6.83</b>
NMRFStereo [13]	4.20	5.10	7.50	3.80	11.92	6.50
NMRFStereo [13] <sup>†</sup>	<b>3.50</b>	<b>4.52</b>	<b>6.43</b>	<b>2.35</b>	<b>9.4</b>	<b>5.24</b>
NMRFStereo [13]*	8.67	7.46	16.36	23.46	34.58	18.11
NMRFStereo [13]* <sup>†</sup>	<b>4.29</b>	<b>4.31</b>	<b>6.96</b>	<b>1.84</b>	<b>7.64</b>	<b>5.01</b>

Table 4. **Ablation study on different models.** NMRFStereo\* refers to NMRFStereo-SwinT. <sup>†</sup> refers to our training strategy.

StereoAnything achieves the lowest error rates on the KITTI 2012 [11], KITTI 2015 [29], and ETH3D [35] datasets, outperforming previous methods. In Table 4, we further present an ablation study that highlights the significant impact of our proposed training strategy, which applied to different stereo backbones yields significant improvement in performance across all datasets. Our training approach consistently delivers significant performance improvements across all datasets, showcasing its versatility and effectiveness. The most striking improvement is seen in the NMRFStereo-SwinT [13] variant, which shows particularly significant improvement, with the mean error reduced from 18.11 to 5.01. This notable gain is attributed to the increased data scale, which allows the SwinTransformer [26] backbone to unlock its full potential.

### 6.4. Ablation Studies

In this section, we are going to ablate our StereoAnything framework, showing in detail how different datasets – labeled and pseudo-labeled – combinations impact the final results.

#### 6.4.1 Training on single labeled stereo datasets.

As shown in Table 6, fine-tuning on synthetic datasets such as Sintel [3], FallingThings [40] and Tartanair [42] generally leads to improved performance over the baseline. However, fine-tuning on certain datasets like Argoverse [7]

Mix	KITTI12 [11]			KITTI15 [29]			Middlebury [34]		ETH3D [35]		DrivingStereo [48]			Mean	Rank
	D1	EPE	Rank	D1	EPE	Rank	Bad2.0	Rank	Bad1.0	Rank	D1	EPE	Rank		
SF [27]	8.67	1.67	-	7.46	1.52	-	16.36	-	23.46	-	34.58	10.53	-	18.11	-
MIX 1	4.65	1.19	9	6.01	1.40	9	10.63	9	12.02	8	9.31	2.17	2	8.52	9
MIX 2	4.11	1.04	7	5.19	1.25	7	8.83	8	10.52	7	<b>8.93</b>	2.19	1	7.52	6
MIX 3	4.46	1.11	8	5.33	1.26	8	7.64	6	7.81	5	33.91	6.40	9	11.83	8
MIX 4	3.79	0.91	5	4.38	1.04	5	7.92	7	10.37	6	24.01	4.57	8	10.09	7
MIX 5	3.73	0.90	3	4.81	1.08	6	7.02	4	12.20	9	22.50	4.15	7	10.05	5
MIX 6	3.75	0.79	4	4.29	1.02	4	6.90	3	6.99	3	11.81	2.60	4	6.74	4
MIX 7	3.64	0.78	2	4.28	1.01	3	<b>6.60</b>	1	7.50	4	9.54	2.20	3	<b>6.31</b>	1
MIX 8	3.81	0.79	6	4.21	1.01	2	6.76	2	<b>4.02</b>	1	15.09	4.82	6	6.78	3
MIX 9	<b>3.55</b>	0.77	1	<b>3.70</b>	0.95	1	7.08	5	6.26	2	11.87	3.22	5	6.49	2

Table 5. **Cross-domain evaluation on different combinations training datasets.** The different MIX setups are explained in Table 7.

Dataset	K12	K15	Midd	E3D	DS	Mean	Rank
SF [27]	8.67	7.46	16.36	23.46	34.58	18.11	-
SF→ST [3]	6.09	6.28	19.28	6.18	37.90	15.15	7
SF→FT [40]	4.28	4.23	13.17	27.93	23.21	14.56	4
SF→Arg [7]	46.10	50.49	45.26	61.21	48.98	50.41	11
SF→VK2 [4]	<b>3.96</b>	<b>4.00</b>	22.23	73.78	53.27	31.45	9
SF→Tar [42]	4.16	4.71	13.95	<b>5.25</b>	47.04	15.02	6
SF→I2K [2]	<b>13.33</b>	<b>15.21</b>	11.75	11.23	23.02	14.91	5
SF→U4K [38]	8.68	6.90	44.98	64.51	72.84	39.58	10
SF→CRE [23]	8.01	6.18	13.73	5.75	37.33	14.20	3
SF→SP [28]	6.59	6.23	16.04	6.96	41.01	15.37	8
SF→DS [18]	<b>11.84</b>	<b>15.36</b>	12.84	5.32	24.74	14.02	2
SF→Carla	4.65	6.01	<b>10.63</b>	12.02	<b>9.31</b>	<b>8.52</b>	1

Table 6. **Cross-domain evaluation when fine-tuning on different single training sets.** Relative to baseline (top row), **green/red** indicates performance improvement/decline. **Bold:** Best.

and UnrealStereo4K [38] results in significantly degraded performance, with mean metric increasing to 50.41% and 39.58%, respectively. This suggests that these datasets may not provide sufficient diversity or introduce biases hindering the model’s generalization of different scenarios. In contrast, our proposed dataset, StereoCarla, demonstrates superior generalization capabilities. Fine-tuning on StereoCarla yields the lowest mean metric of 8.52%. Notably, it performs excellently on DrivingStereo [48] with a D1-all metric of 9.31%, highlighting its effectiveness in capturing real-world driving scenarios. In summary, the choice of fine-tuning dataset plays a crucial role in the generalization ability of stereo-matching models. Datasets that closely mimic the diversity and complexity of real-world environments, such as our StereoCarla, significantly enhance performance across multiple benchmarks.

#### 6.4.2 Training on mixed labeled stereo datasets.

In the mixed experiments, we begin with our StereoCarla dataset, as it achieved the best performance in the previous experiment. Then, similar to [31], we sequentially add other datasets to the mixed dataset according to the ranking results in Table 6.

Table 5 and Table 7 show the detailed performance re-

Mix	Carla	DY	CRE	FT	I2K	Tar	ST	SP	VK2
MIX 1	✓								
MIX 2	✓	✓							
MIX 3	✓	✓	✓						
MIX 4	✓	✓	✓	✓					
MIX 5	✓	✓	✓	✓	✓				
MIX 6	✓	✓	✓	✓	✓	✓			
MIX 7	✓	✓	✓	✓	✓	✓	✓		
MIX 8	✓	✓	✓	✓	✓	✓	✓	✓	
MIX 9	✓	✓	✓	✓	✓	✓	✓	✓	✓

Table 7. **Combinations of labeled stereo datasets.**

sults across these benchmarks for each mix configuration. Notably, the initial combinations (MIX 1 to MIX 3) bring significant improvements in D1 metrics, particularly on KITTI benchmarks. This improvement demonstrates the effectiveness of our StereoCarla dataset as a robust starting point, providing a strong foundation for generalization. As we progress from MIX 4 to MIX 7, incorporating more datasets leads to further performance gains, with MIX 7 yielding the lowest mean error across all tested datasets, achieving a mean D1 error of 6.31, which is the best performance among all configurations. Interestingly, MIX 9, which includes the maximum number of datasets, shows slightly diminished performance compared to MIX 7 in terms of mean error. This suggests that simply adding more datasets may introduce variations that do not always translate into higher accuracy across all benchmarks. These results underscore the importance of carefully selecting and balancing the training datasets to optimize model generalization for diverse real-world scenarios.

#### 6.4.3 Training on pseudo stereo datasets.

As shown in Table 8, we first validate the impact of using different monocular depth estimation models to generate pseudo stereo data on the BDD100k [52] dataset. Fine-tuning on the stereo datasets synthesized using MiDas [31], DepthAnytingV1 [49] (DAv1), and DepthAnytingV2 [50] (DAv2) leads to competitive results, demonstrating the effectiveness of using monocular depth models for



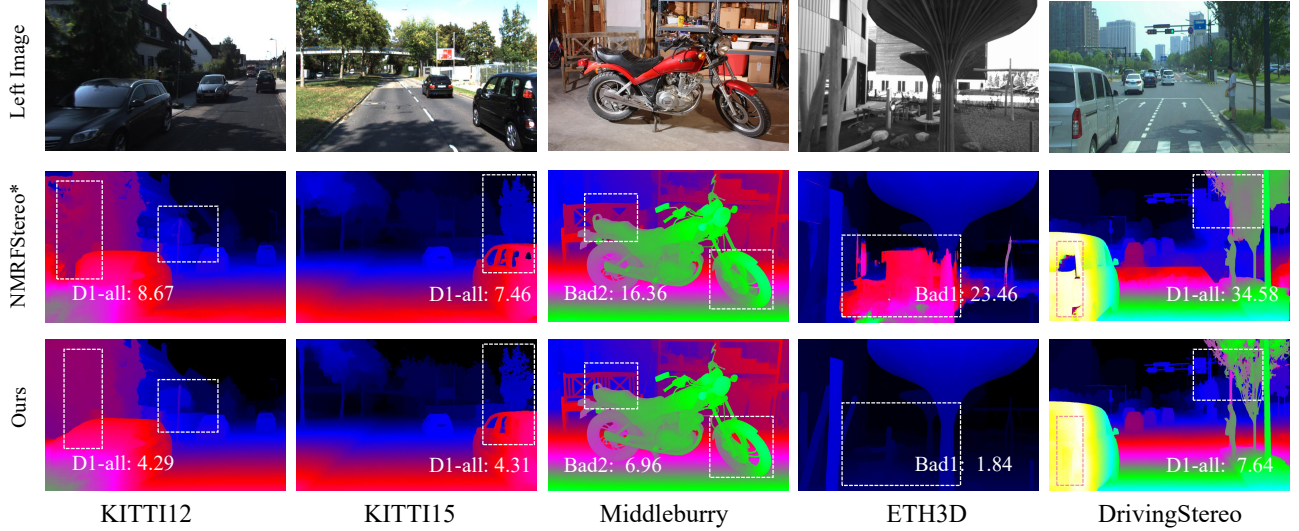


Figure 4. Qualitative results on five unseen datasets. NMRFStereo\* refers to NMRF-Stereo-SwinT [13].

Method	K12	K15	Midd	E3D	DS	Mean
MiDas [31]	4.21	4.23	12.04	4.70	9.22	6.88
DAv1 [49]	4.01	3.98	12.08	4.48	<b>8.81</b>	6.67
DAv2 [50]	<b>3.69</b>	<b>3.87</b>	<b>11.75</b>	<b>3.92</b>	9.55	<b>6.56</b>

Table 8. Ablation study of different monocular depth estimation methods.

pseudo stereo data generation. Specifically, the synthesized data from DAv2 [50] outperforms other monocular methods across all benchmarks.

Then, we evaluate the impact of using different monocular datasets on the performance of the pseudo stereo data generation, based on the DAv2 [50] model. As shown in Table 9, the Google Landmarks [45] achieves the best performance overall, with a mean metric of 5.91. The slightly worse performance of ImageNet21K [32] (21K) and LSUN [51] compared to the GL [45] dataset can be attributed to the lower resolution, which is smaller than our model’s input size. During the process, we resized the images of 21K [32] and LSUN [51] to fit the input size of our model before running the monocular model to estimate depth, followed by generating the pseudo stereo pairs. This resizing process might have led to a loss of fine details, thereby affecting the quality of the generated depth and resulting in slightly lower performance compared to GL [45].

#### 6.4.4 Training on labeled and pseudo stereo datasets.

As shown in Table 10, combining the MIX7 labeled data with pseudo-stereo data from the GoogleLandmarks [45] dataset (denoted as M7+GL-62k) results in further per-

Dataset	K12	K15	Midd	E3D	DS	Mean
SF [27]	8.67	7.46	16.36	23.46	34.58	18.11
LSUN [51]	4.27	4.17	11.88	3.91	10.04	6.85
21K [32]	4.10	4.43	10.44	4.25	9.08	6.46
BDD [52]	3.69	<b>3.87</b>	11.75	3.92	9.55	6.56
PL [61]	<b>3.78</b>	3.91	10.41	3.65	9.19	6.19
GL [45]	3.86	3.98	<b>9.48</b>	<b>3.26</b>	<b>8.97</b>	<b>5.91</b>

Table 9. Ablation study of using pseudo-stereo generated from different datasets.

Dataset	K12	K15	Midd	E3D	DS	Mean
SF [27]	8.67	7.46	16.36	23.46	34.58	18.11
MIX7	<b>3.64</b>	4.28	<b>6.60</b>	7.50	9.54	6.31
GL [45]	3.86	<b>3.98</b>	9.48	3.26	8.97	5.91
M7+GL	4.29	4.31	6.96	<b>1.84</b>	<b>7.64</b>	<b>5.01</b>

Table 10. Cross-domain evaluation combines mix labeled stereo and pseudo-stereo generated from different datasets.

mance gains, achieving the lowest mean metric of 5.01. This combination benefits from both the diversity of labeled stereo data and the robust, diverse depth signals from GoogleLandmarks [45]. These results suggest that combining labeled stereo datasets with high-quality pseudo-stereo data can significantly enhance the generalization capability of stereo models. The diverse, complementary strengths of labeled and pseudo-stereo datasets allow the model to effectively learn detailed and generalized disparity features, ultimately leading to robust performance across various real-world scenarios.

## 6.5. Qualitative Results

In Figure 4, we present the qualitative results of Stereo Anything on five previously unseen datasets. Our model demonstrates strong robustness across various domains, including both indoor and outdoor scenes. Compared to the baseline model, NMRF-Stereo-SwinT [13], our approach consistently produces more accurate disparity maps, as indicated in the visualizations. This qualitative analysis underscores the model’s strong generalization capabilities and its ability to perform well across domains with substantial visual and environmental diversity, validating its effectiveness and potential for real-world stereo-matching applications.

## 7. Conclusion

In this paper, we introduce StereoAnything, a highly practical solution for robust stereo matching. We built a new synthetic dataset to better generalize across different scenarios and enhance the performance, called StereoCarla. Compared to existing datasets, it features unique view angles and baselines. Then, we investigated the effectiveness of labeled stereo datasets and pseudo stereo datasets generated using monocular depth estimation models to enhance stereo model generalization. Our experiments demonstrate that the quality and diversity of the datasets play a critical role in achieving robust stereo-matching performance across different domains. As a result, our StereoAnything achieves competitive performance across various benchmarks and real-world scenarios. These findings underscore the potential of hybrid training strategies that incorporate diverse data sources to enhance stereo model robustness, paving the way for future advancements in stereo matching.

**Acknowledgements.** This work was supported by the National Natural Science Foundation of China under Grant 62373356 and the Open Projects Program of the State Key Laboratory of Multimodal Artificial Intelligence Systems.

# Stereo Anything: Unifying Stereo Matching with Large-Scale Mixed Data

## Supplementary Material

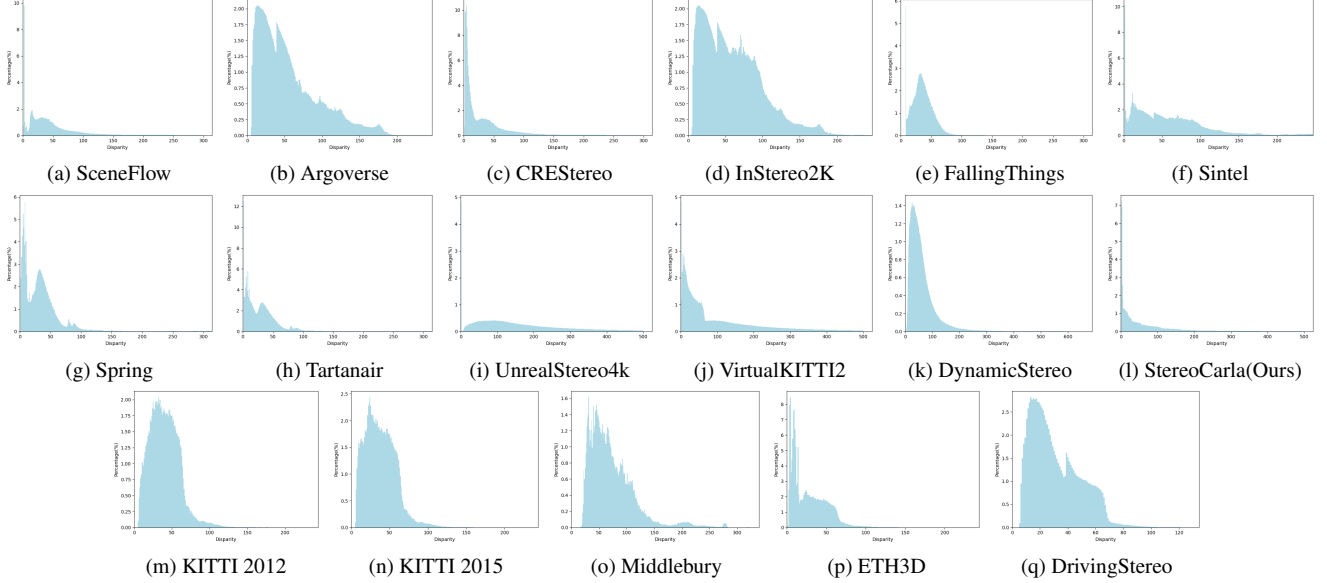


Figure 5. **Disparity distribution across different datasets.** We plot the percentage of pixels at different disparities over single datasets.

## 8. Disparity Distribute

Figure 5 plots the different disparity distributions in each existing labeled stereo dataset, highlighting the diversity in the range and frequency of disparities present. The figure presents the percentage of pixels at different disparity levels for well-known datasets.

## 9. More Implementation Details

Given the relatively low resolution of ImageNet21K, we resize the images while preserving their original aspect ratio to facilitate training on pseudo stereo datasets. Specifically, we ensure that the width is at least 768 pixels and the height is at least 384 pixels. This resizing strategy helps preserve the important visual features in the images while maintaining a resolution suitable for effectively training our model. The resolution of the input image is  $352 \times 640$ .

## 10. More Details about StereoCarla

Table 11 shows the number of samples collected across different towns under various camera configurations. Figure 6 illustrates the left and right images at varying baselines, the corresponding disparity, and diagrams from various angles. These visualizations help in understanding how different baselines affect the stereo image pairs and the resulting disparity, providing insight into the geometry of the captured scenes.

	town01	town02	town03	town04	town05	town06	town07	town10
<b>normal</b>	11700	12425	12235	12335	12420	12420	11090	12415
<b>roll05</b>	12425	12425	12330	9165	11470	12425	12430	12420
<b>roll15</b>	11750	12410	11475	12410	12415	12350	12380	12420
<b>roll30</b>	12195	12405	11165	12415	11930	12145	12420	9995
<b>pitch00</b>	12375	12410	5280	12375	12410	7450	9795	6490
<b>pitch30</b>	12415	12410	12410	11295	12400	12395	12425	6065

Table 11. **StereoCarla samples distribution.** Number of Samples Collected Across Different Towns and Camera Configurations.

## 11. Limitations and Future Works

Currently, our model is trained using over 2 million images. Although, in the current stage, this is sufficient to achieve unprecedented generalization performance, in the future, we plan to incorporate more unsupervised monocular data to train a more robust and effective model, further enhancing its performance and generalization capabilities.

## 12. More Qualitative Results

We present comprehensive qualitative results from five unseen test sets. Specifically, Figure 7 corresponds to KITTI 12, Figure 8 corresponds to KITTI 15, Figure 9 corresponds to Middlebury, Figure 10 corresponds to ETH3D, and Figure 11 corresponds to DrivingStereo. We compare our results with the state-of-the-art NMRFStereo model. Our method demonstrates higher disparity accuracy and greater robustness compared to NMRFStereo, indicating the effectiveness of our approach across diverse datasets.



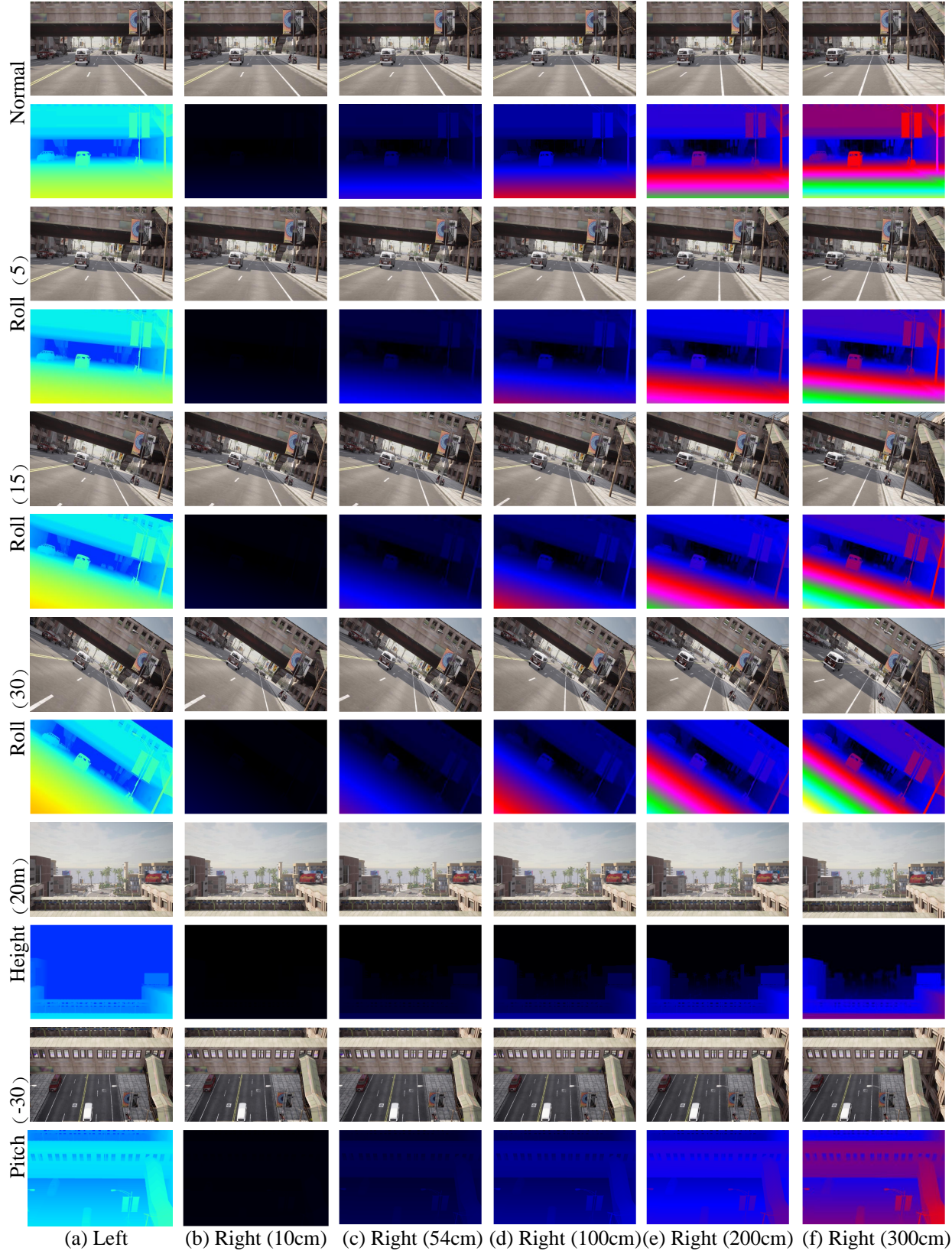


Figure 6. **Overall of StereoCarla datasets.** The first row illustrates the left-eye image (1st column) and the right-eye image at varying baselines (2nd - 6th columns). The second row showcases the depth map (1st column) and corresponding disparity maps (2nd - 6th columns).

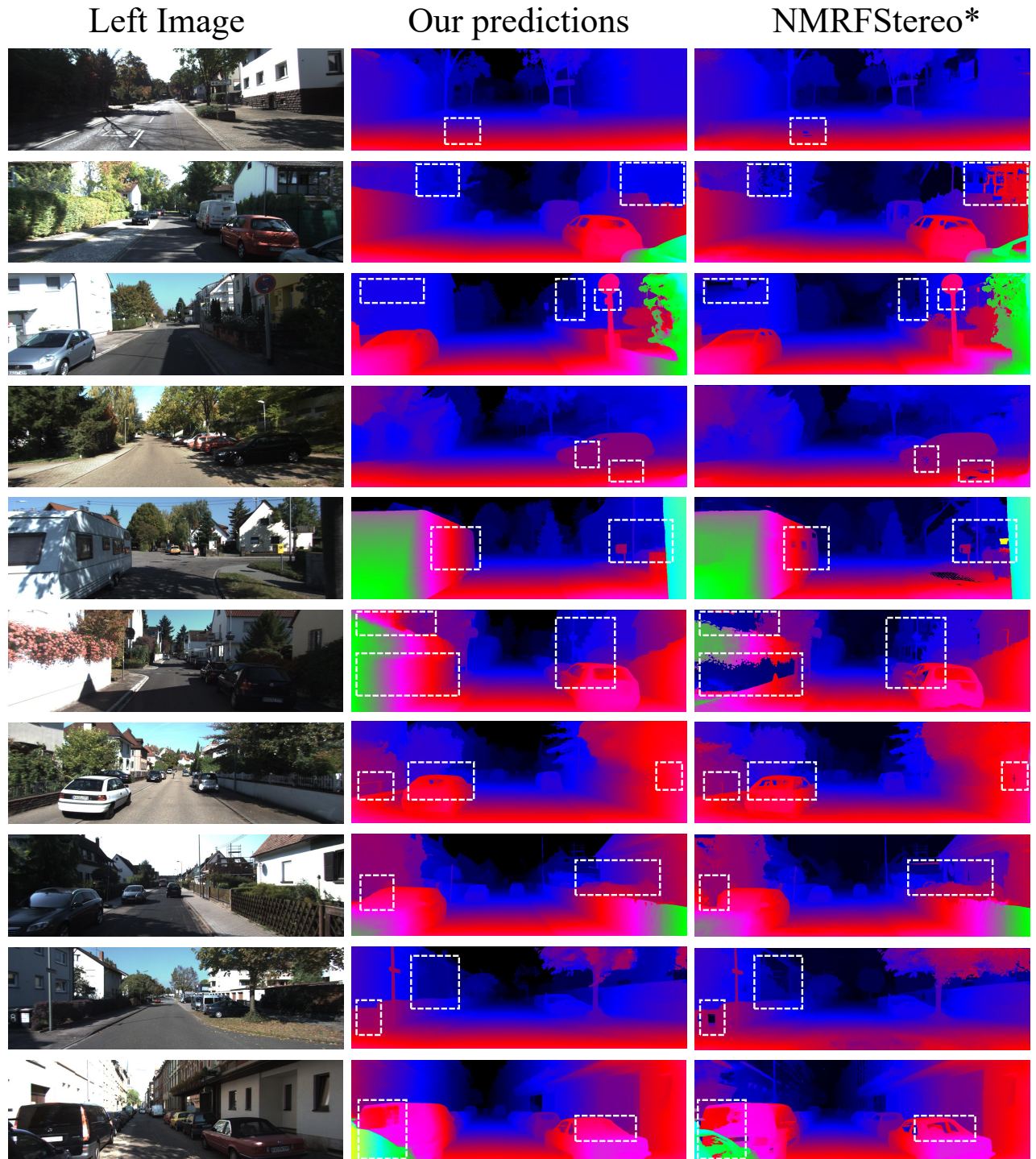


Figure 7. **Qualitative results on KITTI12.** NMRFStereo\* refers to NMRF-Stereo-SwinT.



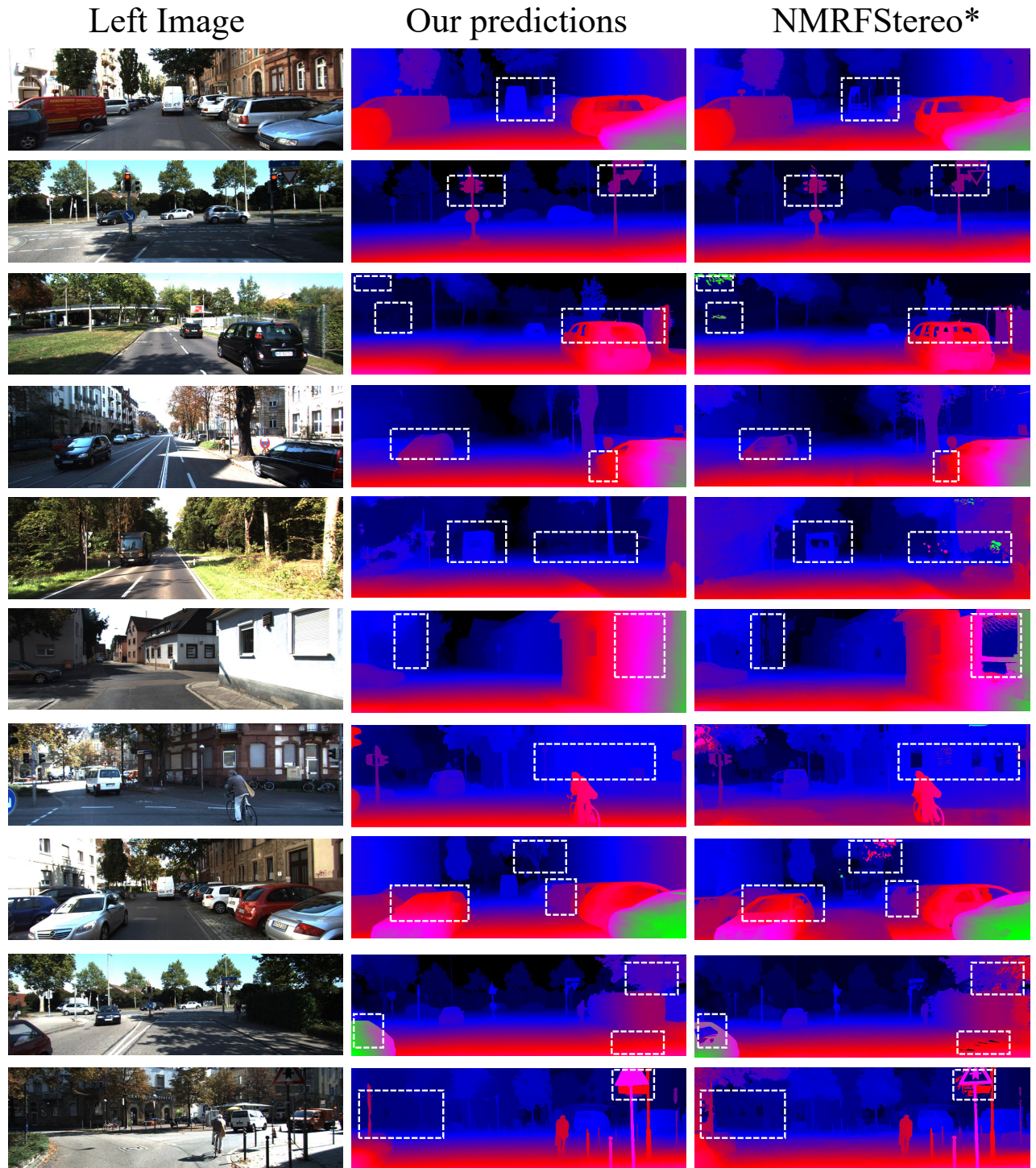


Figure 8. **Qualitative results on KITTI15.** NMRFStereo\* refers to NMRF-Stereo-SwinT.



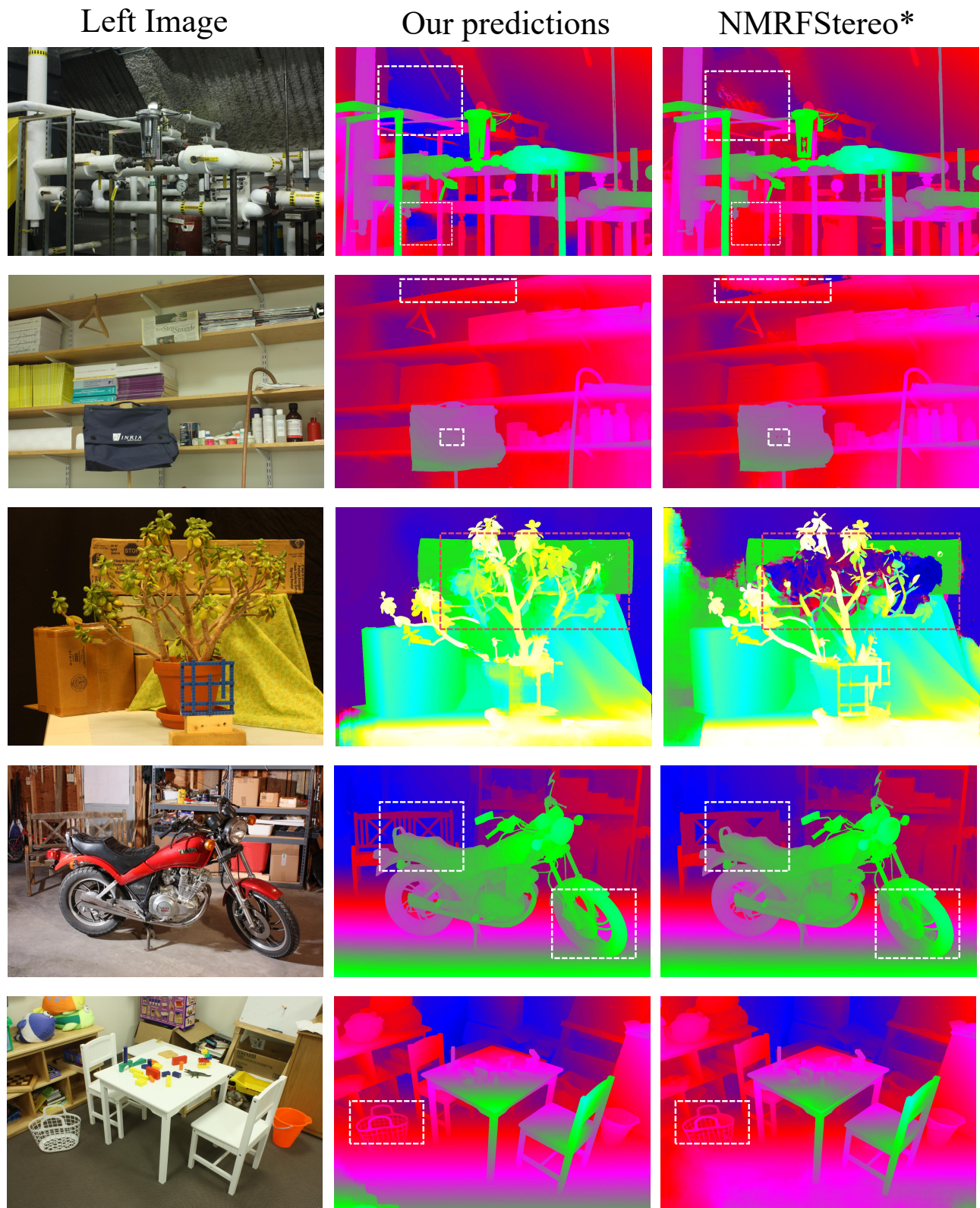


Figure 9. **Qualitative results on Middlebury.** NMRFStereo\* refers to NMRF-Stereo-SwinT.

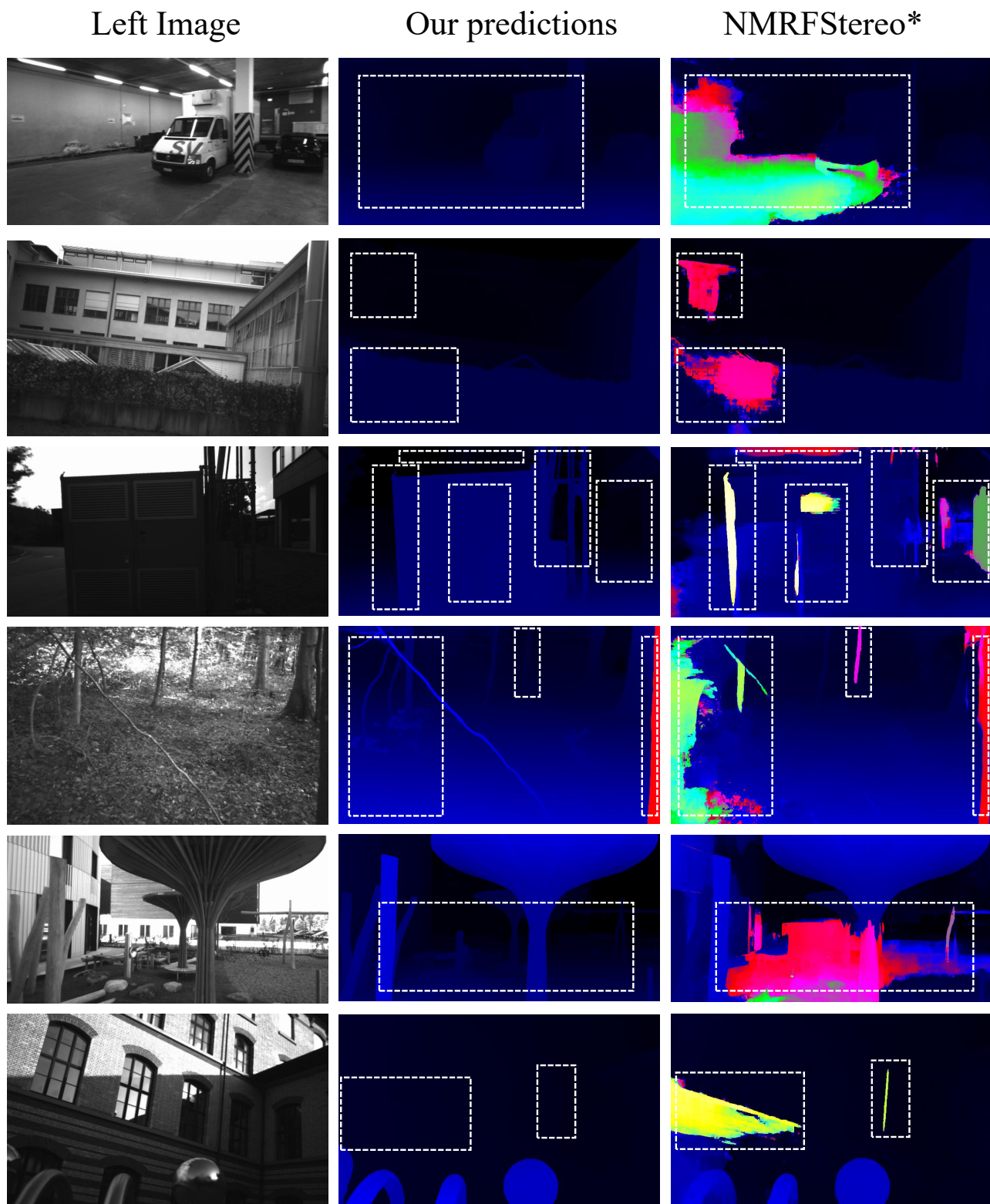


Figure 10. **Qualitative results on ETH3D.** NMRFStereo\* refers to NMRF-Stereo-SwinT.



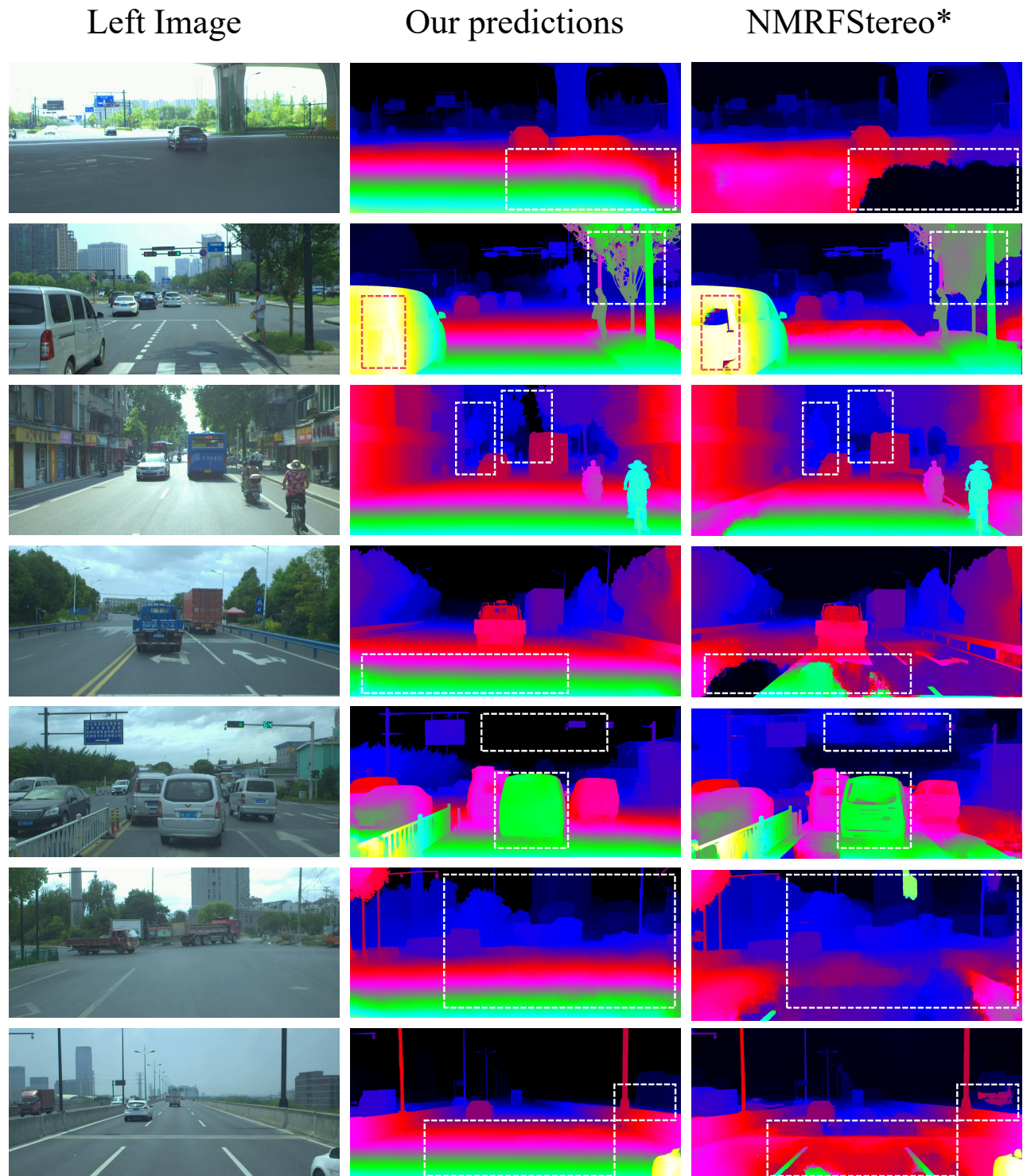


Figure 11. **Qualitative results on DrivingStereo.** NMRFStereo\* refers to NMRF-Stereo-SwinT.



## References

- [1] Antyanta Bangunharcana, Jae Won Cho, Seokju Lee, In So Kweon, Kyung-Soo Kim, and Soohyun Kim. Correlate-and-excite: Real-time stereo matching via guided cost volume excitation. In *IROS*, 2021. 6
- [2] Wei Bao, Wei Wang, Yuhua Xu, Yulan Guo, Siyu Hong, and Xiaohu Zhang. Instereo2k: a large real dataset for stereo matching in indoor scenes. *Science China Information Sciences*, 2020. 3, 7
- [3] Daniel J Butler, Jonas Wulff, Garrett B Stanley, and Michael J Black. A naturalistic open source movie for optical flow evaluation. In *ECCV*, 2012. 3, 6, 7
- [4] Yohann Cabon, Naila Murray, and Martin Humenberger. Virtual kitti 2. *arXiv preprint arXiv:2001.10773*, 2020. 3, 7
- [5] Changjiang Cai, Matteo Poggi, Stefano Mattoccia, and Philippos Mordohai. Matching-space stereo networks for cross-domain generalization. In *3DV*, 2020. 2
- [6] Jia-Ren Chang and Yong-Sheng Chen. Pyramid stereo matching network. In *CVPR*, 2018. 2, 5, 6
- [7] Ming-Fang Chang, John Lambert, Patsorn Sangkloy, Jagjeet Singh, Slawomir Bak, Andrew Hartnett, De Wang, Peter Carr, Simon Lucey, Deva Ramanan, et al. Argoverse: 3d tracking and forecasting with rich maps. In *IROS*, 2019. 3, 6, 7
- [8] Tianyu Chang, Xun Yang, Tianzhu Zhang, and Meng Wang. Domain generalized stereo matching via hierarchical visual transformation. In *CVPR*, 2023. 2
- [9] Xuelian Cheng, Yiran Zhong, Mehrtash Harandi, Yuchao Dai, Xiaojun Chang, Hongdong Li, Tom Drummond, and Zongyuan Ge. Hierarchical neural architecture search for deep stereo matching. In *NeurIPS*, 2020. 2
- [10] Alexey Dosovitskiy, German Ros, Felipe Codevilla, Antonio Lopez, and Vladlen Koltun. CARLA: An open urban driving simulator. In *Proceedings of the 1st Annual Conference on Robot Learning*, pages 1–16, 2017. 4
- [11] Andreas Geiger, Philip Lenz, and Raquel Urtasun. Are we ready for autonomous driving? the kitti vision benchmark suite. In *CVPR*, 2012. 1, 3, 4, 6, 7
- [12] Xiaodong Gu, Zhiwen Fan, Siyu Zhu, Zuozhuo Dai, Feitong Tan, and Ping Tan. Cascade cost volume for high-resolution multi-view stereo and stereo matching. In *CVPR*, 2020. 6
- [13] Tongfan Guan, Chen Wang, and Yun-Hui Liu. Neural markov random field for stereo matching. In *CVPR*, 2024. 2, 5, 6, 8, 9
- [14] Xiaoyang Guo, Kai Yang, Wukui Yang, Xiaogang Wang, and Hongsheng Li. Group-wise correlation stereo network. In *CVPR*, 2019. 2, 6
- [15] Xianda Guo, Juntao Lu, Chenming Zhang, Yiqi Wang, Yiqun Duan, Tian Yang, Zheng Zhu, and Long Chen. Openstereo: A comprehensive benchmark for stereo matching and strong baseline. *arXiv preprint arXiv:2312.00343*, 2023. 1, 6
- [16] Xianda Guo, Chenming Zhang, Dujun Nie, Wenzhao Zheng, Youmin Zhang, and Long Chen. Lightstereo: Channel boost is all your need for efficient 2d cost aggregation. *arXiv preprint arXiv:2406.19833*, 2024. 1
- [17] Heiko Hirschmuller. Stereo processing by semiglobal matching and mutual information. *TPAMI*, 2007. 2
- [18] Nikita Karaev, Ignacio Rocco, Benjamin Graham, Natalia Neverova, Andrea Vedaldi, and Christian Rupprecht. Dynamicstereo: Consistent dynamic depth from stereo videos. In *IROS*, 2023. 1, 2, 3, 7
- [19] Bingxin Ke, Anton Obukhov, Shengyu Huang, Nando Metzger, Rodrigo Caye Daudt, and Konrad Schindler. Repurposing diffusion-based image generators for monocular depth estimation. In *CVPR*, 2024. 1, 2, 3
- [20] Alex Kendall, Hayk Martirosyan, Saumitro Dasgupta, Peter Henry, Ryan Kennedy, Abraham Bachrach, and Adam Bry. End-to-end learning of geometry and context for deep stereo regression. In *ICCV*, 2017. 2
- [21] Alexander Kirillov, Eric Mintun, Nikhila Ravi, Hanzi Mao, Chloe Rolland, Laura Gustafson, Tete Xiao, Spencer Whitehead, Alexander C Berg, Wan-Yen Lo, et al. Segment anything. In *ICCV*, 2023. 1, 3
- [22] Hamid Laga, Laurent Valentin Jospin, Farid Boussaid, and Mohammed Bennamoun. A survey on deep learning techniques for stereo-based depth estimation. *IEEE transactions on pattern analysis and machine intelligence*, 44(4):1738–1764, 2020. 3
- [23] Jiankun Li, Peisen Wang, Pengfei Xiong, Tao Cai, Ziwei Yan, Lei Yang, Jiangyu Liu, Haoqiang Fan, and Shuaicheng Liu. Practical stereo matching via cascaded recurrent network with adaptive correlation. In *CVPR*, 2022. 3, 7
- [24] Lahav Lipson, Zachary Teed, and Jia Deng. Raft-stereo: Multilevel recurrent field transforms for stereo matching. In *3DV*, 2021. 2
- [25] Biyang Liu, Huimin Yu, and Guodong Qi. Graftnet: Towards domain generalized stereo matching with a broad-spectrum and task-oriented feature. In *CVPR*, 2022. 2
- [26] Ze Liu, Yutong Lin, Yue Cao, Han Hu, Yixuan Wei, Zheng Zhang, Stephen Lin, and Baining Guo. Swin transformer: Hierarchical vision transformer using shifted windows. In *ICCV*, 2021. 6
- [27] Nikolaus Mayer, Eddy Ilg, Philip Hausser, Philipp Fischer, Daniel Cremers, Alexey Dosovitskiy, and Thomas Brox. A large dataset to train convolutional

- networks for disparity, optical flow, and scene flow estimation. In *CVPR*, 2016. 1, 3, 6, 7, 8
- [28] Lukas Mehl, Jenny Schmalfluss, Azin Jahedi, Yaroslava Nalivayko, and Andrés Bruhn. Spring: A high-resolution high-detail dataset and benchmark for scene flow, optical flow and stereo. In *CVPR*, 2023. 3, 7
- [29] Moritz Menze and Andreas Geiger. Object scene flow for autonomous vehicles. In *CVPR*, 2015. 1, 3, 4, 6, 7
- [30] Matteo Poggi, Fabio Tosi, Konstantinos Batsos, Philippos Mordohai, and Stefano Mattoccia. On the synergies between machine learning and binocular stereo for depth estimation from images: a survey. *IEEE Transactions on Pattern Analysis and Machine Intelligence*, 44(9):5314–5334, 2021. 3
- [31] René Ranftl, Katrin Lasinger, David Hafner, Konrad Schindler, and Vladlen Koltun. Towards robust monocular depth estimation: Mixing datasets for zero-shot cross-dataset transfer. *TPAMI*, 2020. 1, 2, 3, 5, 7, 8
- [32] Olga Russakovsky, Jia Deng, Hao Su, Jonathan Krause, Sanjeev Satheesh, Sean Ma, Zhiheng Huang, Andrej Karpathy, Aditya Khosla, Michael Bernstein, et al. Imagenet large scale visual recognition challenge. *IJCV*, 2015. 4, 8
- [33] Daniel Scharstein and Richard Szeliski. A taxonomy and evaluation of dense two-frame stereo correspondence algorithms. *IJCV*, 2002. 2
- [34] Daniel Scharstein, Heiko Hirschmüller, York Kitajima, Greg Krathwohl, Nera Nešić, Xi Wang, and Porter Westling. High-resolution stereo datasets with subpixel-accurate ground truth. In *GCPR*, 2014. 3, 4, 6, 7
- [35] Thomas Schops, Johannes L Schonberger, Silvano Galliani, Torsten Sattler, Konrad Schindler, Marc Pollefeys, and Andreas Geiger. A multi-view stereo benchmark with high-resolution images and multi-camera videos. In *CVPR*, 2017. 3, 4, 6, 7
- [36] Zhelun Shen, Yuchao Dai, and Zhibo Rao. Cfnet: Cascade and fused cost volume for robust stereo matching. *arXiv preprint arXiv:2104.04314*, 2021. 2, 6
- [37] Alessio Tonioni, Matteo Poggi, Stefano Mattoccia, and Luigi Di Stefano. Unsupervised adaptation for deep stereo. In *ICCV*, 2017. 2
- [38] Fabio Tosi, Yiyi Liao, Carolin Schmitt, and Andreas Geiger. Smd-nets: Stereo mixture density networks. In *CVPR*, 2021. 3, 7
- [39] Fabio Tosi, Luca Bartolomei, and Matteo Poggi. A survey on deep stereo matching in the twenties. *arXiv preprint arXiv:2407.07816*, 2024. 3, 5
- [40] Jonathan Tremblay, Thang To, and Stan Birchfield. Falling things: A synthetic dataset for 3d object detection and pose estimation. In *CVPRW*, pages 2038–2041, 2018. 3, 6, 7
- [41] Qiang Wang, Shaohuai Shi, Shizhen Zheng, Kaiyong Zhao, and Xiaowen Chu. Fadnet++: Real-time and accurate disparity estimation with configurable networks. *arXiv preprint arXiv:2110.02582*, 2021. 6
- [42] Wenshan Wang, Delong Zhu, Xiangwei Wang, Yaoyu Hu, Yuheng Qiu, Chen Wang, Yafei Hu, Ashish Kapoor, and Sebastian Scherer. Tartanair: A dataset to push the limits of visual slam. In *IROS*, 2020. 3, 6, 7
- [43] Zhenyu Wang, Yali Li, Xi Chen, Ser-Nam Lim, Antonio Torralba, Hengshuang Zhao, and Shengjin Wang. Detecting everything in the open world: Towards universal object detection. In *CVPR*, 2023. 1, 3
- [44] Jamie Watson, Oisín Mac Aodha, Daniyar Turmukhambetov, Gabriel J. Brostow, and Michael Firman. Learning stereo from single images. In *ECCV*, 2020. 1, 2, 5
- [45] T. Weyand, A. Araujo, B. Cao, and J. Sim. Google Landmarks Dataset v2 - A Large-Scale Benchmark for Instance-Level Recognition and Retrieval. In *CVPR*, 2020. 4, 8
- [46] Gangwei Xu, Xianqi Wang, Xiaohuan Ding, and Xin Yang. Iterative geometry encoding volume for stereo matching. In *CVPR*, 2023. 2, 6
- [47] Aimin Yang, Chunying Zhang, Yongjie Chen, Yunxi Zhuansun, and Huixiang Liu. Security and privacy of smart home systems based on the internet of things and stereo matching algorithms. *ISO4*, 2020. 1
- [48] Guorun Yang, Xiao Song, Chaoqin Huang, Zhidong Deng, Jianping Shi, and Bolei Zhou. Drivingstereo: A large-scale dataset for stereo matching in autonomous driving scenarios. In *CVPR*, 2019. 1, 3, 4, 6, 7
- [49] Lihe Yang, Bingyi Kang, Zilong Huang, Xiaogang Xu, Jiashi Feng, and Hengshuang Zhao. Depth anything: Unleashing the power of large-scale unlabeled data. In *CVPR*, 2024. 1, 2, 3, 5, 7, 8
- [50] Lihe Yang, Bingyi Kang, Zilong Huang, Zhen Zhao, Xiaogang Xu, Jiashi Feng, and Hengshuang Zhao. Depth anything v2. *arXiv preprint arXiv:2406.09414*, 2024. 1, 2, 3, 5, 7, 8
- [51] Fisher Yu, Ari Seff, Yinda Zhang, Shuran Song, Thomas Funkhouser, and Jianxiong Xiao. Lsun: Construction of a large-scale image dataset using deep learning with humans in the loop. *arXiv preprint arXiv:1506.03365*, 2015. 4, 8
- [52] Fisher Yu, Haofeng Chen, Xin Wang, Wenqi Xian, Yingying Chen, Fangchen Liu, Vashisht Madhavan, and Trevor Darrell. Bdd100k: A diverse driving dataset for heterogeneous multitask learning. In *CVPR*, 2020. 4, 7, 8

- [53] Jiayi Zeng, Chengtang Yao, Yuwei Wu, and Yunde Jia. Temporally consistent stereo matching. *ECCV*, 2024. [2](#)
- [54] Feihu Zhang, Victor Prisacariu, Ruigang Yang, and Philip H.S. Torr. Ga-net: Guided aggregation net for end-to-end stereo matching. In *CVPR*, 2019. [2](#)
- [55] Feihu Zhang, Xiaojuan Qi, Ruigang Yang, Victor Prisacariu, Benjamin Wah, and Philip Torr. Domain-invariant stereo matching networks. In *ECCV*, 2020. [2](#), [6](#)
- [56] Guoxuan Zhang, Jin Han Lee, Jongwoo Lim, and Il Hong Suh. Building a 3-d line-based map using stereo slam. *IEEE Transactions on Robotics*, 2015. [1](#)
- [57] Jiawei Zhang, Xiang Wang, Xiao Bai, Chen Wang, Lei Huang, Yimin Chen, Lin Gu, Jun Zhou, Tatsuya Harada, and Edwin R Hancock. Revisiting domain generalized stereo matching networks from a feature consistency perspective. In *CVPR*, 2022. [2](#)
- [58] Jiawei Zhang, Jiahe Li, Lei Huang, Xiaohan Yu, Lin Gu, Jin Zheng, and Xiao Bai. Robust synthetic-to-real transfer for stereo matching. In *CVPR*, 2024. [2](#)
- [59] Youmin Zhang, Matteo Poggi, and Stefano Mattoccia. Temporalstereo: Efficient spatial-temporal stereo matching network. *IROS*, 2023. [2](#)
- [60] Yongjian Zhang, Longguang Wang, Kunhong Li, Yun Wang, and Yulan Guo. Learning representations from foundation models for domain generalized stereo matching. In *ECCV*, 2024. [2](#)
- [61] Bolei Zhou, Agata Lapedriza, Aditya Khosla, Aude Oliva, and Antonio Torralba. Places: A 10 million image database for scene recognition. *TPAMI*, 2017. [4](#), [8](#)